Journal of Applied Polymer Science

Thermogravimetric study of thermal degradation of polyetherimide

Sonia Zaragoza,[1] Ana Álvarez,[1] Begoña Álvarez,[1] Jorge López-Beceiro,[1] Salvador Naya,[1] Patricia Forcén,[2] Ramón Artiaga[1]

[1]Escola Politécnica Superior, University of A Coruña, 15403 Ferrol, Spain
[2]SABIC, Crta. Cartagena-Alhama de Murcia km. 13, La Aljorra, Spain
Correspondence to: R. Artiaga (E-mail: ramon.artiaga@udc.es)

ABSTRACT: Thermal stability in nonoxidizing atmosphere of a polyetherimide (PEI) is investigated by thermogravimetry (TG). It is observed that thermal degradation of this product consists of two overlapping processes, which are conveniently separated by fitting the TG curves to mixtures of generalized logistic functions. Thus, each process is represented by a single function. The analysis of the fitting parameter values obtained for the main degradation process in different isothermal and heating ramp conditions allows to obtain insightful kinetic parameters (critical temperature, energy barrier, and reaction-order) which allow to make predictions in both isothermal and nonisothermal contexts. There is a minimum temperature for each process to occur and a ramp-energy barrier related to the process rate. In the ramp context, the values of these two parameters explain that, although one process starts at lower temperature, it proceeds at a very low rate until reaching temperatures at which the other process goes much faster. © 2015 Wiley Periodicals, Inc. J. Appl. Polym. Sci. **2015**, *132*, 42329.

KEYWORDS: degradation; kinetics; thermogravimetric analysis

Received 31 October 2014; accepted 5 April 2015
DOI: 10.1002/app.42329

INTRODUCTION

Thermogravimetric analysis (TG) is frequently used to evaluate the thermal stability of polymers and composites[1–4] and to perform kinetic analysis of the degradation processes. Most of the methods used for determining the kinetic parameters of physico-chemical processes from thermal analysis data can be classified in one of these two approaches: model fitting and model-free procedures.

The model fitting approach, in principle, assumes a fixed mechanism throughout the reaction with a constant activation energy. A limitation that was reported for this method is that the complex reactions cannot be modeled with reasonable accuracy. This procedure involves the fitting of conversion-time data or conversion-rate of conversion-time data to some models to determine reaction orders, rate constants, and the activation energy.[5] The goodness of fit can be improved by introducing additional parameters, although it may compromise its physical significance. Model-free kinetics (MFK) performs an isoconversional analysis on data taken at three or more heating rates, where activation energy is allowed to vary with temperature.[6] Thus, model-free methods allow for more than one mechanism during the course of reaction. A main disadvantage is that a reaction model is usually needed for a complete kinetic description.[7,8] Independently of which of these two approaches, model fitting or model-free, is used, it is almost universally assumed an Arrhenius dependence of the reaction rate on temperature.

The polymer studied here, poly(ether imide), poly[2,2 -bis(3,4-dicarboxyphenoxy)phenylpropane-2-phenylenediimide], (PEI), whose chemical structure is depicted in Figure 1, is an amorphous engineering thermoplastic manufactured by Sabic (R) offering enhanced flow and a glass transition temperature of about 217°C.

PEI brings outstanding elevated thermo oxidative stability,[9–11] high strength and stiffness, broad chemical resistance, exceptionally low smoke generation, and inherent flame retardancy. It is one of the candidate materials for energy storage. Thus, a complete kinetic description allowing to predict lifetimes in different thermal conditions would be of high interest. Thermal degradation mechanism and kinetics of PEI were investigated by means of thermogravimetry (TG) and pyrolyzer instruments hyphenated to infrared spectrophotometer, gas chromatography, or mass spectroscopy.[1–3] The chemical results are highly valuable and menachisms were proposed to explain the chemical results. The first results allowed to tentatively propose that PEI is thermally decomposed by two routes, an ether-bond breaking mechanism and a carboxyl-induced chain breaking mechanism.[1] Further studies concluded that the major mechanisms in this two-stage pyrolysis consisted of

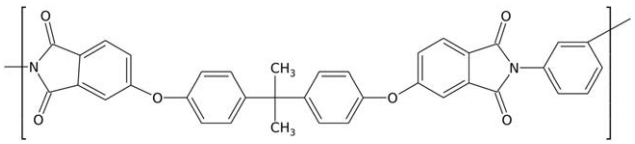

Figure 1. Chemical structure of PEI.

main-chain random scission followed by carbonization.[3] These reports included kinetic analysis based on model fitting to a classical reaction order model and on MFK methods, including Ozawa's, Friedman's, and Kissinger's methods.[12–14] Those methods, which assume an Arrhenius dependence of the reaction rate on the temperature, have been routinely applied in many kinetic studies. Nevertheless, it was not conveniently tested that these models accurately reproduce the degradation processes. The model fitting approach was validated by comparing the results obtained at a single heating rate with those obtained by MFK methods.[1] Nevertheless, MFK does not provide a complete kinetic description and, as mentioned before, a reaction model is usually needed for a complete kinetic description. On the other hand the isoconversional methods did produce an almost constant activation energy for a range of conversion between 0.1 and 0.6 and, although not evident, the authors also claimed that a constant value is obtained between 0.8 and 1.[2] Nevertheless, when that activation energy values were used, assuming a reaction order model, the calculated curves did not match the experimental curves.[2] Both the lack of quality of the fitting and the lack of constancy of the activation energy are indications that the process is not perfectly reproduced by those models. On the other hand, the authors proposed a new kinetic model, based on logistic functions, which generally results in superior quality of fittings than those obtained with Arrhenius-based models. This new model will be applied to the thermogravimetric thermal degradation data of PEI with the aim of checking if it can accurately reproduce its kinetics and, if so, to obtain insightful kinetic parameters (critical temperature, energy barrier and reaction-order) which allow to make predictions in both isothermal and nonisothermal contexts. The approach used for this model is based on other developments of the authors[15–17] and consists of fitting thermogravimetric curves to mixtures of generalized logistic functions. Some simplifications of the model can be done when working with TG data:[17] there is no need of baseline subtraction; the first derivative of a generalized logistic function can fit DTG curves. The generalized logistic function, also known as Richards' curve, is a flexible sigmoid function that was initially used to model the "S-shaped" behavior of growth of some populations. It has been widely used and its application has been expanded to a range of fields, including biology, chemistry, sociology, and statistics.

It was demonstrated that these functions represent a non-Arrhenius reaction order model. This model has a very singular feature: a critical temperature, T_c, which represents the lower limit for the degradation to take place. It has also an energy barrier, E_{iso}, which should not be compared with the activation energy obtained from Arrhenius-based models because, the fact of including or not the T_c factor, leads to completely different values of the energy barrier.

EXPERIMENTAL

Thermogravimetric experiments were conducted in a SDT 2960 simultaneous thermal analyzer, manufactured by TA Instruments. The instrument was calibrated according to manufacturer recommendations. PEI, in the form of pellets, was provided by Sabic (R). Samples of about 9 mg were cut-off from the pellets. A first set of experiments consisted of linear heating ramps at 2, 5, 10, 20, 30, and 40°C min^{-1} from room temperature to 850°C with a 100 mL min^{-1} purge of N_2. A second set consisted of several isotherms at 470°C, 471°C, 473°C, and 476°C. The heating rate from room temperature to the isothermal temperature was 5°C min^{-1}. The 5°C min^{-1} heating rate was chosen based on previous trials with the same instrument. With higher heating rate the overheating would be higher. But, using a lower heating rate would increase the degradation before reaching isothermal conditions. The experiments were manually stopped when, after the maximum of the DTG peak, the mass loss rate was close to zero. Since the results of the previous tests suggested that two processes are overlapping, a new test was designed to verify how both processes could be separated. That test consisted of a 5°C min^{-1} heating ramp to 473°C followed by an isothermal step until constant mass is observed, and then cooling to room temperature and re-heating at 20°C min^{-1} to 800°C.

Fitting to a Mixture of Logistics

Time derivatives of generalized logistic functions will be used to represent the rate of single mass loss processes, both in ramp or in isotherm:

$$y_{ramp}(t) = \frac{c_{ramp} \cdot b_{ramp} \cdot \exp\left(-b_{ramp} \cdot \left(m_{ramp} - t\right)\right)}{\left[1+\tau \cdot \exp\left(-b_{ramp} \cdot \left(m_{ramp} - t\right)\right)\right]^{(1+\tau)/\tau}} \quad (1)$$

$$y_{iso}(t) = \frac{c_{iso} \cdot b_{iso} \cdot \exp\left(-b_{iso} \cdot \left(m_{iso} - t\right)\right)}{\left[1+\tau \cdot \exp\left(-b_{iso} \cdot \left(m_{iso} - t\right)\right)\right]^{(1+\tau)/\tau}} \quad (2)$$

Although formally equivalent, isothermal, and nonisothermal logistic parameters are not the same. The m_{iso} and m_{ramp} parameters represent the time measured from the beginning of the experiment, isothermally or in ramp, to the instant where the maximum mass loss rate is observed. Similarly, b_{iso} and b_{ramp} are related to the rate of the process in isothermal and ramp conditions, respectively (in both cases higher values of b correspond to faster processes). The c_{iso} and c_{ramp} parameters represent the peak area and are related to the mass loss produced in each degradation step. The other parameter, τ, accounts for the asymmetry and is related to a reaction order ($n = 1 + \tau$).[16,18]

As it can be observed in Figure 2, the shape of DTG curves obtained in ramp suggests that these curves could be represented by mixtures of two time derivative generalized logistics. Accordingly, each of the single DTG curves obtained in ramp was fitted by a mixture of two logistic components:

$$y_{ramptotal}(t) = y_{ramp1}(t) + y_{ramp2}(t) \quad (3)$$

where $y_{ramptotal}(t)$ represents the DTG curve and $y_{ramp1}(t)$ and $y_{ramp2}(t)$ are described by eq. (1). The fitting was optimized by minimizing the sum of squared residuals (SSR) which is a method that has been widely used.[19] Fityk software was chosen to perform that task.[20]

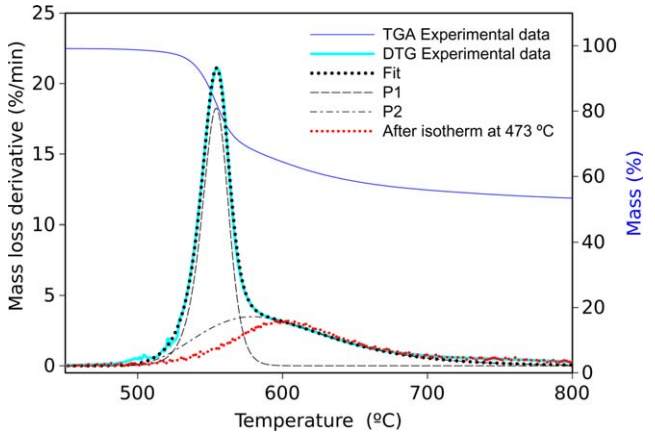

Figure 2. TG and DTG curves resulting from a 20°C min^{-1} heating ramp performed ona pristine sample (cyan) and a DTG curve obtained at the same heating rate from a sample previously subjected to an isothermal treatment at 473°C (red). The DTG from the pristine sample is separated into two logistic components (P1 and P2). [Color figure can be viewed in the online issue, which is available at wileyonlinelibrary.com.]

Obtaining very good fittings with a two-component model supports the two-stage pyrolysis reported by other authors.[2,3,21] Studies of the pyrolysis products suggest that the main degradation step, referred here as P1, basically consists of random scission of hydrolyzed imide, ether, and isopropylidene groups, producing CO, CO_2, and phenol as the major products. Simultaneously, chain transfer reactions would produce a partially carbonized solid residue. The second pyrolysis stage, P2, would mainly consist of the decomposition of the partially carbonized solid residue and remaining imide groups producing CO and CO_2 as the major product along with benzene and a small amount of benzonitrile.[3] What the P1 and P2 represent are the two degradation processes, independently of the number of mechanisms involved in each process. The two logistic components in which the DTG curve was split in Figure 2 are associated to the first and second pyrolysis stages and thus respectively labelled as P1 and P2.

According to Figure 2, the process represented by the P1 component is dominant in the range of temperature where the isothermal tests are performed. A new test is performed in order to verify that assumption: a 5°C min^{-1} heating ramp to 473°C followed by an isothermal step until a constant mass is observed for five minutes, and then cooling to room temperature and re-heating at 20°C min^{-1} to 800°C. Figure 2 plots an overlay of the DTG curve resulting from this final re-heating step on that obtained with a fresh sample at 20°C min^{-1}. It can be observed how the re-heating curve basically corresponds to the P2 component of the fresh sample, although, as expected, a part of this component disappeared during the pre-isothermal treatment. That part of the P2 component is little in comparison with the P1 component, which disappeared as a whole. This means that for the isothermal tests performed in the 470–476°C range, the minority contribution of the P2 process could be neglected. Thus, fitting of each isothermal curve will make use of only one logistic component, represented by eq. (2). On the other hand, only the data acquired after the isothermal step was well established are taken into account for the fitting procedure.

Kinetic Analysis

While the generalized logistic function was proposed in 1959 as a flexible growth function for empirical use,[22] it was not until our recent work that a true kinetic approach was used to interpret the processes that can be described by that function.[15,16,18] A complete kinetic description should consider both isothermal and nonisothermal situations.

a. The nonisothermal case

Equation (1) can be expressed as functions of the conversion of the process, α:

$$y_{ramp}(t,\ \alpha) = c_{ramp} \cdot b_{ramp} \cdot \exp\left(-b_{ramp} \cdot \left(m_{ramp} - t\right)\right) \cdot (1-\alpha)^{1+\tau} \tag{4}$$

Based on this expression the model can be understood as a reaction order model, being the reaction order represented by $1 + \tau$.[15]

According to our previous results, the b_{ramp} parameter verifies the following relation:[16]

$$b_{ramp} = \frac{E_{ramp}}{R \cdot t_{pramp} \cdot T_c} \tag{5}$$

where T_c is the critical temperature for the process to occur, t_{pramp} represents the time elapsed from the instant where temperature reached a critical value, T_c, to the instant where the maximum rate of change is observed, m_{ramp}. E_{ramp} is an apparent energy barrier, and R is the gas constant. Obviously if b_{ramp} values are plotted against $1/(R\ t_{pramp}\ T_c)$ the result must be a straight line crossing at the origin and its slope is E_{ramp}.

Since

$$t_{pramp} = \frac{T_p - T_c}{HR} \tag{6}$$

where T_p is the peak temperature and HR the heating rate, it is possible to obtain the optimal values of E_{ramp} and T_c parameters that verify eq. (5). Consequently, the b_{ramp} values obtained from the fittings of single DTG curves obtained in ramp practically fall into a straight line crossing at the origin, as depicted in Figure 3. The resulting values of E_{ramp}

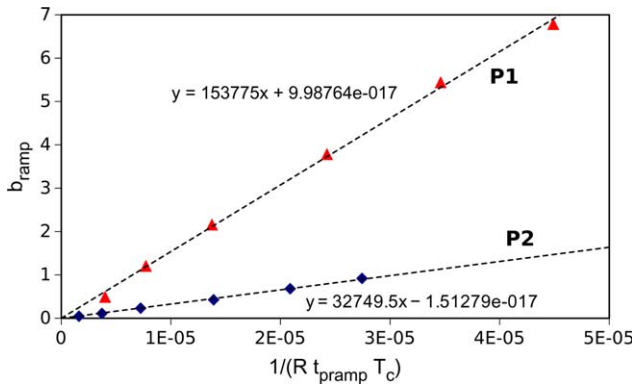

Figure 3. Plots of the b_{ramp} values versus $1/(R\ t_{pramp}\ T_c)$ corresponding to the two overlapping processes. [Color figure can be viewed in the online issue, which is available at wileyonlinelibrary.com.]

Table I. E_{ramp} and T_c Obtained for the Processes P1 and P2

	P1	P2
E_{ramp} (kJ mol^{-1})	154	33
T_c (°C)	410.3	250.6

and T_c are displayed in Table I. It is important to note that E_{ramp} does not represent a true energy barrier because the values of b_{ramp} and t_{pramp} involved in eq. (5) were derived from nonisothermal conditions and, thus, are not associated to specific temperatures. Nevertheless, a higher value of E_{ramp} is associated to faster processes in ramp. The T_c value obtained for P1 is higher than that obtained for P2. It explains that, although the P2 process starts at a lower temperature, in practice, both processes proceed at an almost negligible rate up to about 520°C. Then, the P1 process is clearly dominant, and only when this process is almost completed, the P2 process becomes dominant. Nevertheless, if P2 can start at lower temperature than P1, as suggested by their respective T_c values, then the P2 process would not be limited to the partially carbonized structure with the remaining imide groups but would also involve part of the unreacted material.

In order to verify that the small deviations from linearity observed in Figure 3 are not relevant for the quality of the fittings, new fittings of the DTG curves to eq. (1) were performed making use of the b_{ramp} values that exactly fall in the line for corresponding t_{pramp} values (it implies to lock pairs of b_{ramp} and m_{ramp} values). The goodness of the fittings practically did not change, being the coefficient of determination, R^2, higher than 0.99 in all cases. The parameter values resulting from the fittings are displayed on Table II. Figure 4 shows how the fittings of the DTG curves by the model perfectly match the experimental curves. The scale does not allow to distinguish between the two processes as in Figure 2.

Figure 5 shows how the plots of the exponential term of eq. (1) versus temperature cross at T_c.

b. The isothermal case

As explained above in Figure 2, there is a minority contribution of the P2 process can be neglected for kinetic analysis of the isothermal tests performed in the 470–476°C range. This is a consequence of the T_c_P2 value being lower than that corresponding to T_c_P1 and practically prevents a separated study of the P2 component in its original form in the sample. It is neither T_c nor E_{ramp} by themselves but the combination of both which determines how fast a given process may proceed in a heating ramp. Nevertheless, if the material was kept for a longtime at a temperature in the middle of both T_cs, only the P2 process would take place. On the other hand, according to Figure 2, it is easy to imagine that, except for the case of isotherms at temperatures in the middle of both T_cs, the P1 process would determine the structural fail because of thermal degradation. Thus, the isothermal study was limited to the P1 process and the isothermal curves were fitted to eq. (2) using only the data acquired since the isothermal step was well established. The optimal parameter values are displayed on Table III. The coefficient of determination is close to 1. Figure 6 shows the DTG curves obtained at different isothermal temperatures and their corresponding fittings.

Using an equivalent approach to that used in the nonisothermal case, eq. (2)2 can be expressed as a reaction order model, being the reaction order represented by $1+\tau$[16]

$$y_{iso}(t,\ \alpha) = c_{iso} \cdot b_{iso} \cdot \exp(-b_{iso} \cdot (m_{iso} - t)) \cdot (1-\alpha)^{1+\tau} \quad (7)$$

and the b_{iso} parameter verifies this relation:

$$b_{iso} = \frac{E_{iso}}{R \cdot t_{piso} \cdot T_c} \quad (8)$$

where t_{piso} represents the time elapsed from the instant where temperature reached a critical T_c value to the instant where the maximum rate of change is observed, m_{iso}. Assuming a relatively fast heating rate from below T_c to the isothermal temperature, that time basically (although not completely) corresponds to isothermal conditions. E_{iso} is a true energy barrier and can be obtained as the slope of the straight line obtained when plotting b_{iso} versus $1/(R\ t_{piso}\ T_c)$, as indicated in Figure 7. Provided the T_c value obtained from ramp, E_{iso} can be then calculated from a single isothermal experiment. This experiment should be

Table II. Parameter Values Obtained from the Fittings of DTG Curves Obtained in Ramp to eq. (3)

	P1						P2					
	Heating rate (°C min^{-1})						Heating rate (°C min^{-1})					
	2	5	10	20	30	40	2	5	10	20	30	40
c_t (wt %)	21.89	22.14	22.15	22.40	22.36	22.27	21.06	21.09	21.39	20.80	21.50	21.93
τ	3.01	1.79	1.69	1.47	1.29	1.31	6.54E-03	6.93E-02	1.57E-02	9.52E-05	1.67E-04	1.18E-07
b_{ramp} (min^{-1})	0.61	1.19	2.11	3.73	5.32	6.90	0.05	0.12	0.24	0.46	0.68	0.90
m_{ramp} (min)	0.61	1.19	2.11	3.73	5.32	6.90	0.05	0.12	0.24	0.46	0.68	0.90
Tp (°C)	497.3	522.1	537.0	554.2	562.6	567.0	530.4	555.2	564.5	578.9	579.7	584.4

T_p is the temperature at the m_{ramp} instant.

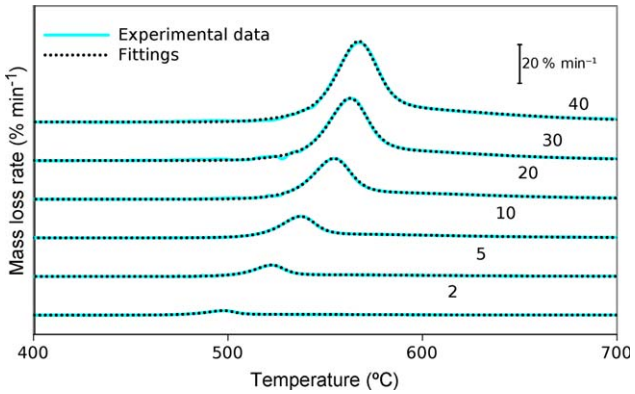

Figure 4. Overlay of the experimental curves and the corresponding fittings. The curves were shifted on the y-axis for easier observation. [Color figure can be viewed in the online issue, which is available at wileyonlinelibrary.com.]

performed at a relatively high temperature (higher b_{iso}) to minimize the effect of any possible experimental error on the slope.[18] A value of 22 kJ mol^{-1} was obtained for the P1 process. This value is very different from others obtained in solid–solid and melting transformations.[15,16,18]

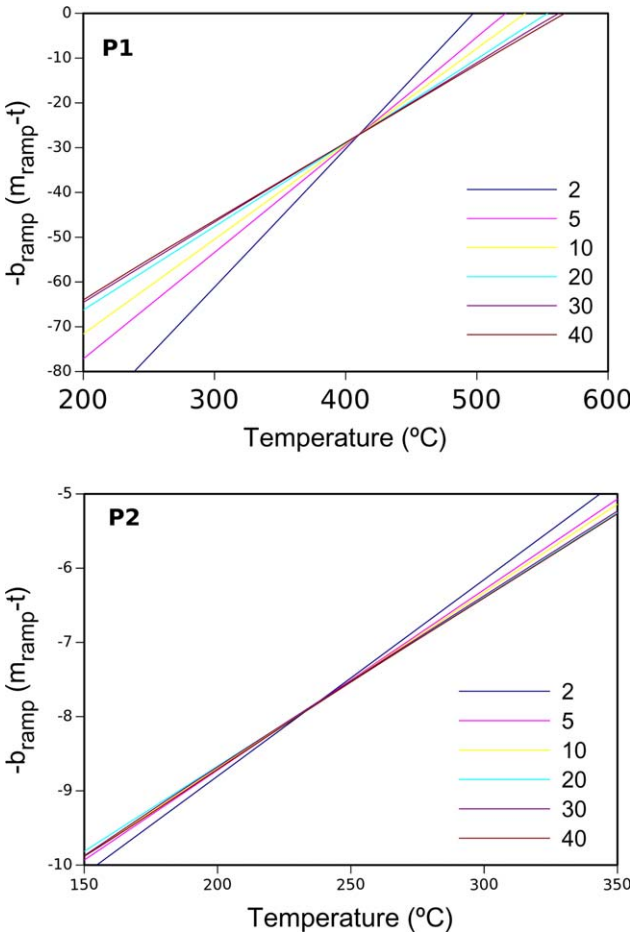

Figure 5. Exponential terms of $y_{ramp1}(t)$ and $y_{ramp2}(t)$ versus temperature obtained at the indicated heating rates. [Color figure can be viewed in the online issue, which is available at wileyonlinelibrary.com.]

Table III. Parameter Values Obtained from the Fittings of DTG Isothermal Curves for the P1 Process

	Isothermal Temperature (°C)			
	470	471	473	476
c_t (wt %)	23.15	26.02	23.26	25.36
τ	1.20	3.49	2.68	3.56
b_{iso} (min^{-1})	0.12	0.19	0.20	0.23
m_{iso} (min)	121.31	119.17	115.82	112.47

Parameter Trends

In order to make reliable predictions of the degradation rate in different thermal conditions, it is necessary to know how the most insightful parameters of eqs. (1)s and (2) vary with temperature. The c parameter represents the amount of sample involved in each degradation process and is not dependent on the temperature or the heating rate. Thus, it can be considered a constant except if the sample was previously degraded. The b_{iso} parameter is related to t_{piso} through eq. (8) and the b_{ramp} parameter is related to t_{pramp} through eq. (5). Since E_{iso}, E_{ramp}, and T_c were previously determined, the trends of the peak time in isothermal and ramp conditions can be easily calculated if the b_{iso} and b_{ramp} trends are known. It was already reported that the peak time, t_{piso}, follows a trend that can be described by this equation:[16]

$$t_{piso} = t_{Tb} \cdot \exp\frac{(T-T_b)}{(T_c-T)} \tag{9}$$

where T_c is the critical temperature obtained from the ramp experiments and T_b, t_{Tb}, and b_{Tb} are fitting parameters. T_b simply represents a higher reference temperature at which the peak time would take a given value, t_{Tb}. Figure 8 shows the t_{piso} values versus isothermal temperature.

On the other hand, b_{iso} and b_{ramp} are related through this expression:[16]

$$\frac{b_{iso}}{b_{ramp}} = \frac{t_{pramp}}{t_{piso}} \cdot \frac{E_{iso}}{E_{ramp}} \tag{10}$$

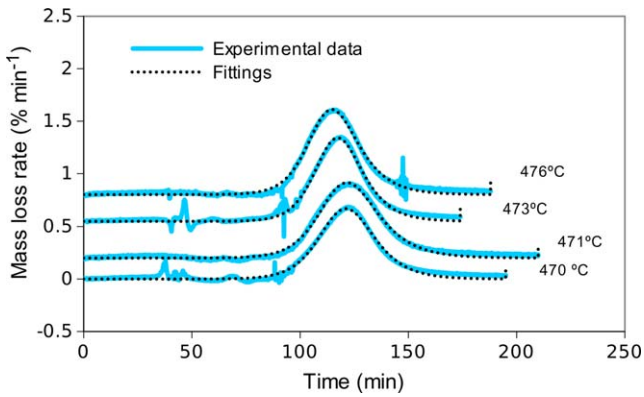

Figure 6. Plots of the DTG curves obtained from isothermal experiments and the corresponding fittings. [Color figure can be viewed in the online issue, which is available at wileyonlinelibrary.com.]

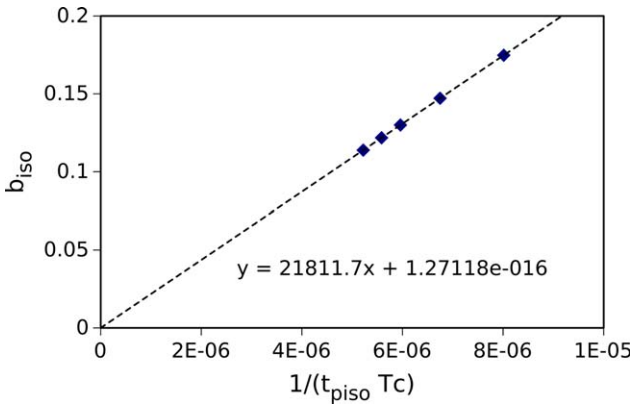

Figure 7. Plots of the b_{iso} parameter values versus 1/(R t_{piso} T_c) obtained for the P1 process. [Color figure can be viewed in the online issue, which is available at wileyonlinelibrary.com.]

And t_{pramp} is related to the peak temperature, T_p, through eq. (6). Figure 9 shows how T_p-T_c for both processes, P1 and P2, follows power trends.

On the other hand, the τ parameter seeems to have a subtle effect, affecting only the symmetry of the peak. According to Figures 10 and 11, there is not a clear trend in isothermal nor in ramp experiments. In general, for heating rate situations, an average value of 1.5 can be assumed for P1. P2 could only be conveniently evaluated in heating rate mode and a value of 0 was found. For the isothermal context, values of 1.5 and 0 are also good. Reaction orders greater than 2 for a single reactant may be difficult to justify and one might have to consider whether a model invoking the control of an inhibitive intermediate might be applicable.[23]

Considerations on the Physical Meaning and Comparison to Arrhenius-Based Models

In a previous work of the authors, the generalized logistic model has been described and compared from a statistical point of view with some well-known kinetic models as Avrami– Erofeev, power law, and classical reaction order.[24] That study has indicated that the generalized logistic function can reproduce

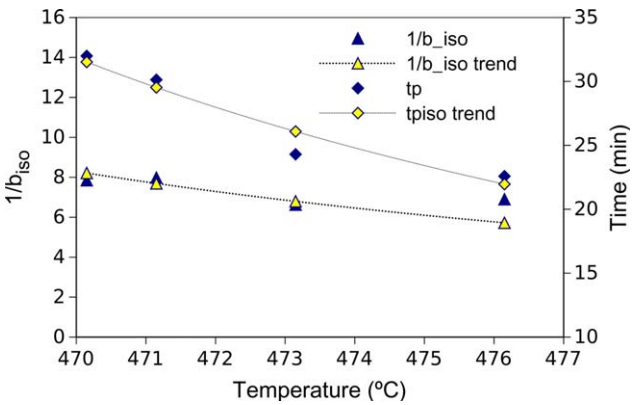

Figure 8. Plots of t_{piso} and of $1/b_{iso}$, obtained from isothermal experiments, versus temperature, and the trend lines, according to eq. (8) and (9), for the P1 process. [Color figure can be viewed in the online issue, which is available at wileyonlinelibrary.com.]

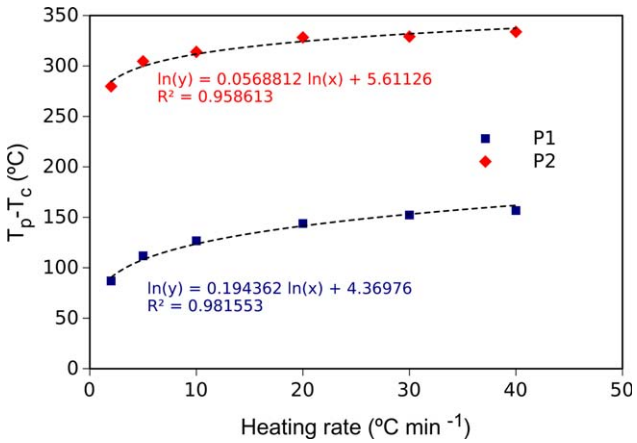

Figure 9. Plots of T_p–T_c versus heating rate for the P1 and P2 processes. [Color figure can be viewed in the online issue, which is available at wileyonlinelibrary.com.]

quite well Arrhenius reaction order processes, eq. (11), except for some combinations of parameter values (n relatively high, combined to a low E/R values, high heating rates, and a low value for the pre-exponential factor):

$$\frac{d\alpha}{dt} = A\exp\left(\frac{-E}{R \cdot T}\right) \cdot (1-\alpha)^n. \qquad (11)$$

where E is the activation energy, α the conversion and n the order of reaction. As one can easily infer, although there are some more or less complex relations, there are not univocal correspondences between the parameters in eq. (7) and (11).

Since many thermal degradation processes are analyzed by Arrhenius-based models, a quick comparison of the performance of one of that models with the one presented here seems convenient. Particularly, activation energy values of 230 kJ mol^{-1}, as determined by Ozawa's method, were reported for the first degradation step of PEI. Making use of that activation energy value, a two-stage model consisting of two Arrhenius reaction order components was proposed to represent the pyrolysis of PEI in helium. That model was reported to be compliant with the experimental data.[2] In order to ensure a fair

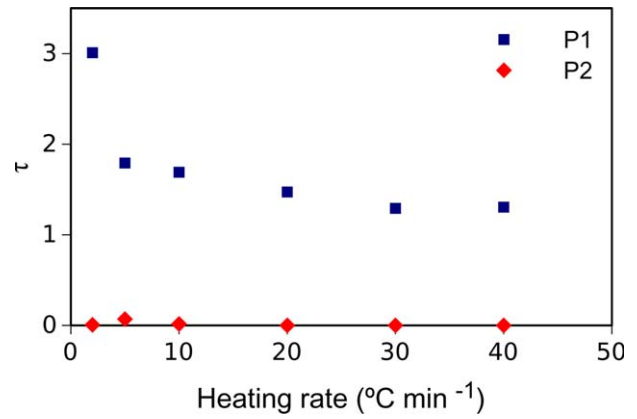

Figure 10. Plot of τ versus the heating rate in nonisothermal experiments for P1 and P2. [Color figure can be viewed in the online issue, which is available at wileyonlinelibrary.com.]

comparison, one of the datasets used in the nonisothermal kinetic analysis section are now fitted by a two Arrhenius reaction order components mixture. The activation energy obtained this way was 259 kJ mol^{-1}, which is in line with the value reported as determined by Ozawa's method. But more important than the degree of compliance with reported values is the ability of the model to represent the process. Figure 12 plots an overlay of the experimental data and the fittings obtained with the method proposed by the authors and a two Arrhenius reaction order components mixture. The quality of fitting obtained with the proposed method is clearly superior to that obtained with the Arrhenius-based one. Additionally, the parameter values obtained with the generalized logistic mixture model agrees with the analysis of data obtained at different heating rates, as discussed in the nonisothermal case section.

One important feature of the model used here is that it does not assume an Arrhenius dependence on the temperature. Instead, there is a critical temperature for each thermal degradation process, which is the minimum temperature below which the process cannot occur. This parameter is crucial in order to obtain good fittings. For example, imposing a zero value for T_c the quality of the fittings would worsen being similar to that obtained with Arrhenius-based models. Thus, although the physical meaning of the energy barrier is similar to the activation energy in Arrhenius-based models, the values cannot be compared between models with different temperature dependences because there is not an univocal correspondence between both parameters. A recent work of the authors compared the energy barrier values obtained for other processes and materials assuming the same model than in the present work.[4] In this context, the true energy barrier value obtained here, 22 kJ mol^{-1}, is of the same order than those obtained for the main degradation step of two acrylic-based copolymers (about 11 kJ mol^{-1}).

As mentioned before, the expressions for isothermal and nonisothermal processes are formally equivalent, but physically different. In isothermal conditions, the model is described by eq. (2), which was used to fit single curves. As a function of the degree of advancement of the process, α, the model can be

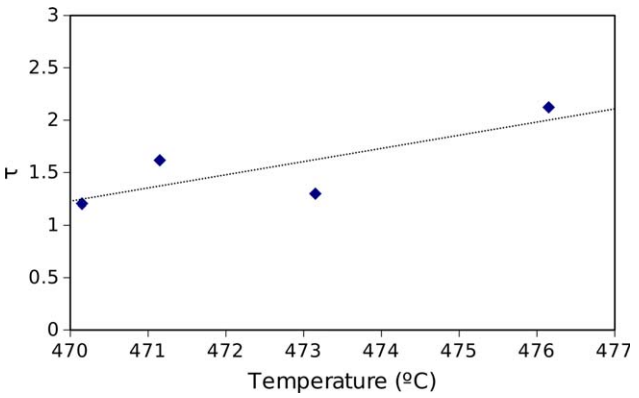

Figure 11. Plot of τ versus the isothermal temperature for P1. [Color figure can be viewed in the online issue, which is available at wileyonlinelibrary.com.]

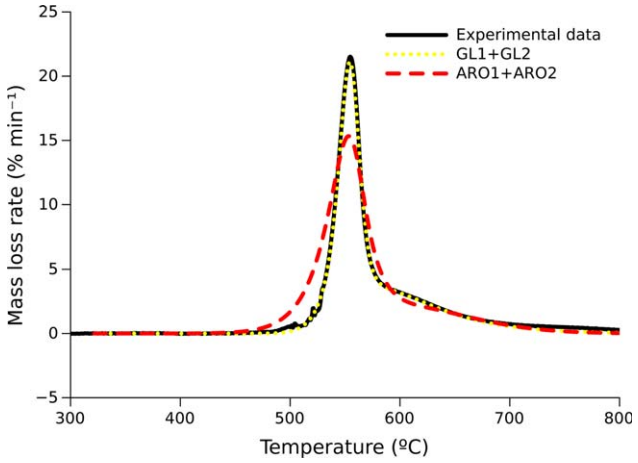

Figure 12. Fittings obtained making use of a mixture of two Arrhenius reaction order (ARO) functions and the proposed generalized logistic (GL) model on a DTG trace obtained at 20 K min^{-1}. [Color figure can be viewed in the online issue, which is available at wileyonlinelibrary.com.]

rewritten as eq. (7), which is clearly a reaction order model, where the reaction order is represented by $1 + \tau$. It also deserves mention that τ is related to the asymmetry of the peak and a perfectly symmetric peak corresponds to $\tau = 1$ (reaction order- = 2). The c parameter represents the peak area, in this case the amount of sample involved in the process, b governs the rate along the process, so that a bigger value of b means a faster process. The m parameter represents the location of the maximum rate on the time axis. In order to clarify the physical meaning of these parameters, the relation described by eq. (8) was introduced. This expression relates the b parameter to three more insightful parameters: the energy barrier, the critical temperature and the peak time. The consistency of this proposal is supported by the alignment of the points in the plot of Figure 7, where the energy barrier is the slope. On the other hand, the critical temperature can be calculated from few nonisothermal experiments. Although the true energy barrier only appears in the isothermal case, the nonisothermal parameters allow to quantify the effect of applying a heating rate by comparison with the isothermal ones.

CONCLUSIONS

In agreement with previous studies, thermal degradation of PEI in nitrogen atmosphere basically consists of two overlapping processes. These processes were conveniently separated by fitting the ramp data to mixtures of generalized logistic functions so that each process is represented by a single function. The parameter values obtained in ramps and isotherms allowed to obtain a complete kinetic description of the main degradation process. There is a slower overlapping process that could not be separately studied in isotherm. The kinetic values were very different from those obtained in other processes.

ACKNOWLEDGMENTS

This work was partially funded by the Spanish Ministerio de Educación y Ciencia MTM2011-22393.

REFERENCES

1. Huang, F.; Wang, X.; Li, S. *Polym. Degrad. Stab.* **1987**, *18*, 247.
2. Perng, L. -H. *J. Polym. Res.* **2000**, *7*, 185.
3. Perng, L. H. *J. Appl. Polym. Sci.* **2001**, *79*, 1151.
4. López-Beceiro, J.; Álvarez-García, A.; Martins, S.; Álvarez-García, B.; Zaragoza-Fernández, S.; Menéndez-Valdés, J.; Artiaga, R. *J. Therm. Anal. Calorim. [Internet]*. **2015**, *119*, 1981 [cited 2015 Feb 9]; Available from: http://link.springer.com/10.1007/s10973-014-4386-y.
5. Brown, ME.; Maciejewski, M.; Vyazovkin, S.; Nomen, R.; Sempere, J.; Burnham, A.; Opfermann, J.; Strey, R.; Anderson, H. L.; Kemmler, A.; Keuleers, R.; Janssens, J.; Desseyn, H. O.; Li, C.-R.; Tang, T. B.; Roduit, B.; Malek, J.; Mitsuhashi, T. *Thermochim. Acta* **2000**, *355*, 125.
6. Vyazovkin, S. Isoconversional kinetics; Elsevier: **2008**, Chapter 13, p 503. Available from: http://linkinghub.elsevier.com/retrieve/pii/S1573437408800167
7. Khawam, A.; Flanagan, D. R. *J. Phys. Chem. B* **2006**, *110*, 17315.
8. Khawam, A.; Flanagan, D. R. *J. Phys. Chem. B* **2005**, *109*, 10073.
9. Gupta, P.; Alam, S. *J. Appl. Polym. Sci.* **2011**, *120*, 2790.
10. Shibata, M.; Fang, Z.; Yosomiya, R. *J. Appl. Polym. Sci.* **2001**, *80*, 769.
11. Crevecoeur, G.; Groeninckx, G. *Macromolecules* **1991**, *24*, 1190.
12. Ozawa, T. *Bull. Chem. Soc. Jpn.* **1965**, *38*, 1881.
13. Friedman, H. L. *J. Polym. Sci. C Polym. Symp.* **1964**, *6*, 183.
14. Kissinger, H. E. *Anal. Chem.* **1957**, *29*, 1702.
15. López-Beceiro, J.; Gracia-Fernández, C.; Gómez-Barreiro, S.; Castro-García, S.; Sánchez-Andújar, M.; Artiaga, R. *J. Phys. Chem. C* **2012**, *116*, 1219.
16. López-Beceiro, J.; Gracia-Fernández, C.; Artiaga, R. *Eur. Polym. J.* **2013**, *49*, 2233.
17. Rios-Fachal, M.; Gracia-Fernández, C.; López-Beceiro, J.; Gómez-Barreiro, S.; Tarrío-Saavedra, J.; Ponton, A.; Artiaga, R. *J. Therm. Anal. Calorim.* **2013**, *113*, 481.
18. López-Beceiro, J.; Fontenot, SA.; Gracia-Fernández, C.; Artiaga, R.; Chartoff, R. *J. Appl. Polym. Sci.* **2014**, n/a.
19. Cao, R.; Naya, S.; Artiaga, R.; García, A.; Varela, A. *Polym. Degrad. Stab.* **2004**, *85*, 667.
20. Wojdyr, M. *J. Appl. Crystallogr.* **2010**, *43*, 1126.
21. Carroccio, S.; Puglisi, C.; Montaudo, G. *Macromol. Chem. Phys.* **1999**, *200*, 2345.
22. Richards, F. J. *J. Exp. Bot.* **1959**, *10*, 290.
23. Vannice, M. A. Kinetics of Catalytic Reactions [Internet]; Springer: New York, **2005** [cited 2014 Oct 26]. Available from: http://site.ebrary.com/id/10229289
24. Tarrío-Saavedra, J.; López-Beceiro, J.; Naya, S.; Francisco-Fernández, M.; Artiaga, R. *J. Therm. Anal. Calorim.* **2014**, *118*, 1253.